Vascular Parameters of Normal Cynomolgus Macaques by Fundus Fluorescence Angiography and Optical Coherence Tomography Angiography

Jingyi Peng
State Key Laboratory of Ophthalmology Zhongshan Ophthalmic center Sun Yat-sen University
Liuxueying Zhong
State Key Laboratory of Ophthalmology Zhongshan Ophthalmic Center Sun Yat-sen University
Li Ma
State Key Laboratory of Ophthalmology Zhongshan Opthalmic Center Sun Yat-Sen University
Jiayi Jin
Sun Yat-Sen University Zhongshan Ophthalmic Center
Yongxin Zheng (fdhqs@126.com)
State Key Laboratory of Ophthalmology, Zhongshan Ophthalmic Center, Sun Yat-Sen University

Research Article

Keywords: Cynomolgus macaques, Vascular, Fundus fluorescence angiography (FFA), Optical coherence tomography angiography (OCT-A), vessel density (VD)

Posted Date: December 13th, 2018

DOI: https://doi.org/10.21203/rs.2.85/v1

Version of Record: A version of this preprint was published on October 11th, 2019. See the published version at https://doi.org/10.1186/s12886-019-1207-x.

Abstract

Background: To provide normal vascular parameters for cynomolgus macaques. Compare the advantages and disadvantages of Fundus fluorescence angiography (FFA) and Optical coherence tomography angiography (OCT-A) in angiography. To establish an eye parameter database for cynomolgus macaques.

Methods: Five normal cynomolgus macaques were studied for the collection of data, with a mean age of 4.6±0.55 years. The Heldelberg Spectralis® HRA+OCT was used to obtain parameters for Fundus fluorescence angiography (FFA). The vessel density was measured using the RTVue XR with AngioVue (software version 2017.1.0.155; Optovue, Inc., Fremont, CA, USA); the scan sizes of the macular and optic discs were 3×3mm and 4.5×4.5mm, respectively.

Results: Cynomolgus macaque's fundus fluorescence angiography had similar stages as those found in humans. Optical coherence tomography can image the superficial, deep capillary plexus and the radial peripapillary capillary network. The highest whole En-face mean vessel density (VD) in the macular area was 68.19±0.75 % in the choroid capillary layer. In both layers of the optic disc, the vessel density in the Nasal quadrant was lower than in the inferior-tempo quadrant.

Conclusions: This is a rare research, where we have collected the normal FFA and the novel OCT-A parameters for cynomolgus macaques. This study provides normal vascular parameters of cynomolgus macaques via Fundus fluorescence angiography (FFA) and Optical coherence tomography angiography (OCT-A), helping to establish an optical parameter database for cynomolgus macaques, promoting choroid-retinopathy research.

Background

Retina plays a vital role in vision. The metabolic activity of retina is higher than other human tissues1,2 and therefore the vascular circulation of retina is complex. A variety of techniques have been used to measure retinal perfusion. Fundus fluorescence angiography (FFA) was routinely used to evaluate retinal vascular retinopathy3 as it could analyze the choroid-retinal vasculature, and show vascular leakage and neovascularization4. However, there are some limitations to this methodology, such as the intravenous injection of contrast agents that can lead to some side-effects5,6. Additionally, FFA images are unable to extract further details of deeper capillary plexus, due to limited depth perception. Optical coherence tomography angiography (OCT-A) is a novel imaging method7, that detects the flow of blood via intrinsic signal, without the requirement of using an intravenous agent. It can visualize and divide the retina into various layers, clearly showing the capillary vessels in each layer. The ability of OCT-A to quantify blood flow and vascular density of the retinal choroidal circulation is essential to the study of global ophthalmology.

Owing to close similarity to humans in optical structure and function, nonhuman primates like cynomolgus macaque serve a crucial role in ophthalmic disease research8-11. The FFA and OCTA vascular parameters for normal humans have been reported before1,12, and researchers have reported the flow perfusion parameters for normal monkeys13. However, there is very little literature available on the vascular density parameters for the macular and optic disc of ocularly normal cynomolgus macaques. Our study aims to evaluate the macular vascular circulation parameters in normal rhesus monkeys using OCTA and FFA, and to compare the advantages and disadvantages of the two techniques in angiography.

Methods

Animals

Data was collected from five normal adult male cynomolgus macaques, with a mean age of 4.6±0.55 years, and a mean weight of 4.44±0.88 kg. The animal production license number was SCXK(YUE)2014-0027 (GuangZhou Blooming-Spring Biological Technology Development Co. Ltd). Before the start of the experiments, all five animals were determined to be ocularly normal and healthy. After these experiments, the animals are in good care and will be used for further research.

Preparation of animal

Animals were anesthetized with an intramuscular Injection (im.) of ZoletilTM50 (VIRBAC S.A.), which is the combination of Tiletamine-Zolazepam (4mg/kg). Anesthesia was maintained during examinations by intravenously injecting supplemental doses of ZoletilTM50 (1/3 of the initial dose) as needed. Body temperature was monitored using a water circulating heating pad at 37℃. Pupils were fully dilated to approximately 9 mm in diameter with Tropicamide Phenylephrine Eye Drops (0.5%, Santen-China, China). Sodium Hyaluronate Eye Drops

(0.3%, Santen-China, China) were used to maintain corneal moisture. A restraining device was used to maintain stable positioning of the animal's eyes and head. The eyelids were opened with a lid speculum.

Acquisition of data

Fundus fluorescence angiography (FFA)

Five cynomolgus macaques were used in this experiment. FFA images were obtained by the Heidelberg Spectralis® HRA+OCT (Heidelberg Engineering, Heidelberg, Germany) in the FA mode. A 24G intravenous indwelling needle was inserted into the ulnar vein of the monkey. The needle was attached to a 1ml syringe containing Fluorescein Sodium Injection (20%, 0.05 ml/kg). The intravenous dye was infused over 3 s. The photographic documentation of the posterior pole and the peripheral retina was conducted over 18 min.

Optical coherence tomography angiography (OCT-A)

Both eyes of the animals were scanned using RTVue XR with AngioVue (software version 2017.1.0.155; Optovue, Inc., Fremont, CA, USA). The scan size for the macular was 3×3mm, and for the optic disc was 4.5mm×4.5mm.

Vessel density (VD) is defined as the percentage area occupied by blood vessels. AngioVue could automatically divide the scanned area of macular into four sections according to vascularity as follows: the superficial layer (upper line: ILM with offset of 3 micron; lower line: IPL with offset of 16 micron), the deep retina layer (upper line: IPL with 16 micron offsets; lower line: IPL with 69 micron offsets), the outer retina layer (upper line: IPL with 69 micron offsets; lower line: REP with offset of 16 micron) and the choroid capillary (upper line: REP with offset of 31 micron; lower line: RPE with offset of 60 micron). The scanned area of vessel density in the optic disc was divided into two sections: the nerve head (upper line: ILM with offset of 0 micron; lower line: ILM with offset of 150 micron) and the radial peripapillary capillary (upper line: ILM with 0 micron offsets; lower line: NFL with 0 micron offsets). A single trained researcher carried out all image acquisition.

The flow density map software AngioAnalytics can automatically evaluate the VD of the scanned area. In the macular area, the inner and outer rings with a diameter of 1 and 3 mm, centered on fovea, divided the scanned area into six sections: fovea, parafovea, temporal (T), superior (S), nasal (N) and inferior (I), where the fovea center was automatically determined from the relevant OCT data. In the optic disc area, a ring with a width of 0.75mm, centering on the disc, automatically divided the scanned area into seven sections: Inside disc (ID), Nasal (N), Inferior nasal (IN), Inferior temporal (IT), Superior temporal (ST), superior nasal (SN) and temporal (T).

Statistical analysis

The test images acquired by FFA and OCT-A were loaded onto Photoshop CS6. The FFA images for the macular and optic disc areas were enlarged and intercepted to match the details seen on the optical coherence tomography angiography images. IBM SPSS statistics version 19.0 (SPSS, Inc. Chicago, USA) was used to analyze the data. The measurements are presented as mean ± standard deviation (SD). The vessel density comparison of different layers and different regions of each layer were analyzed via Bonferroni analysis. The significance adopted was, $P < 0.05$.

Results

Stages of Fundus fluorescence angiography

Human Fundus fluorescence angiography is mainly divided into five stages: early arterial stage, arterial stage, arteriovenous stage, venous stage and later stage. In our study, cynomolgus macaques' FFA images tend to have similarities with the human angiographic stages. As seen in Figure 1, the mean arm-retina circulation time is (5”11±1”35) s and most of the fluorescence dissipation occurs at (17’18±1’21) min.

Vessel density of Fovea and Parafovea region

Fluorescein angiographic imaging of the central macular region easily shows the superficial capillary plexus however it is not capable of imaging it at a greater depth. Figure 2 shows the four levels of choroid-retinal capillary network images from OCT-A, including the superficial layer, the deep retina layer, the outer retina layer, and the choroid-capillary. When comparing whole En-face vessel density among the four layers, the highest VD was shown to be in the Choroid Cap layer. The parafovea region in the outer retina layer on the other hand had the lowest vessel density of (39.60±3.85). The four peripapillary sections of each retinal layer, showed no significant distinctions .

Vessel density of Optic disc and Peripapillary region

When compared to optical coherence tomography, the fluorescein angiographic image of the optic disc and surrounding regions shows the radial peripapillary capillary network less obviously, as shown in Figure3. In Table2, comparing the measurements of two layers, the mean

vessel density of Whole En-face, Inside Disc region and Peripapillary region are distinguishing (P<0.01). The vessel density of the Inside Disc region is higher in the nerve head. In the peripapillary region, the vessel density is much higher in radial peripapillary capillary layer (P<0.01). With regard to the six peripapillary regions of each retinal layer, vessel density in the inferior-tempo section is significantly higher than in the Nasal section (P<0.05) of the Nerve head layer. In the RPC layer, the vessel density is lower in Nasal quadrant than in inferior-tempo and superior-tempo quadrant (P<0.05).

Discussion

Fundus fluorescence angiography (FFA) is a conventional and qualitative technology, used for diagnosis of retinal vascular diseases, such as Diabetic Retinopathy (DR) and Central Retinal Vein Occlusion (CRVO)14,15. With the use of a special intravenous dye, FFA turns out to be one of the most valuable methods to evaluate the retinal vasculature. It is well known that FFA can record the filling process of choroid-retinal vascular and have a wide field of vision. It can analyze the choroid-retinal vascular, show vascular leakage and neovascularization4. In this study, the FFA showed clear images of retinal vascular activity. Fluorescence angiography shows that cynomolgus macaque has similar stages as humans: the early arterial stage (stage before retinal artery filling), arterial stage (where the whole retinal artery is filling), arteriovenous stage (retinal vein laminar flow), venous stage (where the whole retinal vein is filling) and later stage (fluorescence vanished). The mean arm-retina circulation time is (5”11±1”35) s. In humans, the RCT is usually 7”-15”s. This difference may be due to blood vessel diameter and blood flow velocity.

Optical coherence tomography angiography (OCT-A) is a novel imaging method6,16. It developed as an extension of OCT that clearly showed vascular circulation in the retina and choroid17,18. Unlike FFA, OCT-A detects blood flow via intrinsic signal, without the use of any intravenous agents, thereby avoiding any serious side-effects arising from fluorescent dyes. FFA can be time consuming as the spread of the fluorescent agent is limited by the rate of blood flow leading to a long period of time before obtaining any vascular images. OCT-A on the other hand is time-saving owing to quick scanning speeds. It is axiomatic that FFA provides two-dimensional (2D) images of vascular circulations3, limiting depth perception and detailed investigation of vessels4. The development of Optical coherence tomography angiography can solve these problems. OCT-A can visualize the flow and divide the retina into various layers, clearly showing capillary vessels in each layer; not only transparent vessels. Therefore, some deeper capillary plexus can be observed through optical coherence tomography angiography, which is often mistaken for background choroid fluorescence in FFA 4,19. Interestingly, the optical coherence tomography image in which the radial peripapillary capillary network is readily visible and the fluorescein angiographic image in the same region in our study, show considerable similarities with *Richard F*'s research in humans4. No prior research has shown radial peripapillary capillary network by using fluorescein angiography20.

Researchers can quantitatively analyze vessel parameters via high-resolution imaging in OCT-A. Therefore in this study, we further compared the vessel density of macular, optic disc and surrounding regions via OCT-A. There are four levels of choroid-retinal capillary networks in the macular of cynomolgus macaques, including the superficial layer, the deep retina layer, the outer retina layer, and the choroid-capillary. Comparing the whole En-face vessel density among the four layers, the highest was found to be in the Choroid Cap layer. These results are in concordance with *Florence Coscas*' research in humans1. One possible explanation for this maybe that the deep layer is formed by a homogenous capillary vortex21, whereas the superficial layer is formed only by transverse capillaries; additionally, the superficial layer may artificially influence the vessel density assessment of the DCP1. In the fovea area, the vessel density is the lowest, compared to the other sections of the retinal layer, probably due to the fovea avascular zone (FAZ)18.

We found the vessel density of the whole En-face and the Inside Disc section to be higher in the nerve head layer. In contrast, the VD of peripapillary region is much higher in radial peripapillary capillary layer. In both of the optic disc layers, the vessel density in nasal quadrant is lower than inferior-tempo quadrant. Overall, optical coherence tomography can image the radial peripapillary capillary network better. The blood supply associated with early optic disc lesions in glaucoma patients comes from the microcirculation of the posterior ciliary artery, hence the observation of the radial peripapillary capillary layer is beneficial in the early diagnosis of glaucoma22.
Despite the novelty of OCT-A, especially in assessing different diseases23-27, it's still unclear how OCT-A may be used in disease management, especially in animal models. Nowadays, the nonhuman primates, especially cynomolgus macaques, serve a very important role in the research of ophthalmic diseases owing to similarities in optical structure and function with humans8-11. Therefore, fully understanding the traditional FFA and the novel OCT-A parameters and comparing their images can help in establishing these techniques, especially OCT-A, for the diagnosis of disease in animal models.

In conclusion, we evaluated the macular vascular circulation parameters in normal cynomolgus macaques by OCT-A and FFA and compared the advantages and disadvantages of the two techniques in angiography. Furthermore, we analyzed the vessel density parameters of the choroid-retinal vascular. All in all, our research provides normal vascular parameters of cynomolgus macaques, promoting the establishment of an eye parameter database for non-human primates. Our study does have certain limitations that need to be addressed. Such as the

experimental animal used was cynomolgus macaque, and therefore its unclear if these results are applicable to other species. Our future goal is to do an extensive study across different species, comparing the similarities and differences of FFA and OCT-A.

Declarations

Corresponding Author:
Prof. Yong-Xin Zheng, State Key Laboratory of Ophthalmology, Zhongshan Ophthalmic Center, Sun Yat-Sen University, Guangzhou, Guangdong 510060, China (Tel: 86-020-87331537. Email: fdhqs@126.com).

Author Contributions:

Prof. Yong-Xin Zheng had full access to all the data in the study and takes responsibility for the integrity of the data and the accuracy of the data analysis. All authors have read and approved the manuscript.

Study concept and design: JY P, LXY Z, YX Z

Acquisition, analysis, or interpretation of data: JY P, L M, JY J

Drafting of the manuscript: JY P, LXY Z

Critical revision of the manuscript for important intellectual content: JY P, LXY Z, YX Z, L M, JY J

Statistical analysis: J P

Administrative, technical, or material support: JY P, LXY Z, YX Z

Study supervision: LXY Z, YX Z

Competing interests: All authors come from the State Key Laboratory of Ophthalmology, Zhongshan Ophthalmic Center, Sun Yat-Sen University, Guangzhou, Guangdong 510060, China. the author(s) have no potential competing interests.

Funding: This study was supported by the grants from the National Natural Science

Foundation of China (81570839). Funder: Yong-xin zheng.

Ethical approval: Ethical approval was given by the Animal Experimental Ethics Committee of Zhongshan Ophthalmic Center, Sun Yat-sen University, with the following reference number: SYXK(YUE)2016-114. We conscientiously abide by the ethical principles of animal welfare, at any time accepted the Commission's supervision and inspection.

Date availability statements: The datasets generated and analysed during the current study are not available due to that we have further research related to the subject, but are available from the corresponding author on reasonable request.

References

1. Coscas F, Sellam A, Glacet-Bernard A, et al. Normative Data for Vascular Density in Superficial and Deep Capillary Plexuses of Healthy Adults Assessed by Optical Coherence Tomography Angiography. *Invest Ophthalmol Vis Sci.* 2016;57(9):Oct211-223.

2. Buttery RG, Hinrichsen CF, Weller WL, Haight JR. How thick should a retina be? A comparative study of mammalian species with and without intraretinal vasculature. *Vision research.* 1991;31(2):169-187.

3. Novotny HR, Alvis DL. A method of photographing fluorescence in circulating blood in the human retina. *Circulation.* 1961;24:82-86.

4. Spaide RF, Klancnik JM, Jr., Cooney MJ. Retinal vascular layers imaged by fluorescein angiography and optical coherence tomography angiography. *JAMA ophthalmology.* 2015;133(1):45-50.

5. Trindade-Porto C, Alonso-Llamazares A, Robledo T, et al. Fluorescein-induced adverse reaction. *Allergy.* 1999;54(11):1230.

6. Hagag AM, Gao SS, Jia Y, Huang D. Optical coherence tomography angiography: Technical principles and clinical applications in ophthalmology. *Taiwan journal of ophthalmology.* 2017;7(3):115-129.

7. Jia Y, Bailey ST, Hwang TS, et al. Quantitative optical coherence tomography angiography of vascular abnormalities in the living human eye. *Proceedings of the National Academy of Sciences of the United States of America.* 2015;112(18):E2395-2402.

8. Jonas JB, Hayreh SS. Ophthalmoscopic appearance of the normal optic nerve head in rhesus monkeys. *Invest Ophthalmol Vis Sci.* 2000;41(10):2978-2983.

9. Hood DC, Frishman LJ, Saszik S, Viswanathan S. Retinal origins of the primate multifocal ERG: implications for the human response. *Investigative Ophthalmology & Visual Science.* 2002;43(5):1673.

10. Wilsey LJ, Reynaud J, Cull G, Burgoyne CF, Fortune B. Macular Structure and Function in Nonhuman Primate Experimental Glaucoma. *Invest Ophthalmol Vis Sci.* 2016;57(4):1892-1900.

11. T Michael N, Kim CBY, Munsey KM, Dashek RJ, Hoeve JNV. Regional choroidal blood flow and multifocal electroretinography in experimental glaucoma in rhesus macaques. *Investigative Ophthalmology & Visual Science.* 2014;55(12):7786-7798.

12. Yu J, Jiang C, Wang X, et al. Macular perfusion in healthy Chinese: an optical coherence tomography angiogram study. *Invest Ophthalmol Vis Sci.* 2015;56(5):3212-3217.

13. Li J, Yang YQ, Yang DY, et al. Reproducibility of Perfusion Parameters of Optic Disc and Macula in Rhesus Monkeys by Optical Coherence Tomography Angiography. *Chinese medical journal.* 2016;129(9):1087-1090.

14. Bajwa A, Aman R, Reddy AK. A comprehensive review of diagnostic imaging technologies to evaluate the retina and the optic disk. *International ophthalmology.* 2015;35(5):733-755.

15. Hong BK, Nazari KH, Rao NA. Role of ultra-widefield fluorescein angiography in the management of uveitis. *Canadian Journal of Ophthalmology Journal Canadien Dophtalmologie.* 2013;48(6):489-493.

16. Ishibazawa A, Nagaoka T, Takahashi A, et al. Optical Coherence Tomography Angiography in Diabetic Retinopathy: A Prospective Pilot Study. *American Journal of Ophthalmology.* 2015;160(1):35-44.

17. Cohen SY, Miere A, Nghiem-Buffet S, Fajnkuchen F, Souied EH, Mrejen S. Clinical applications of optical coherence tomography angiography: What we have learnt in the first 3 years. *European journal of ophthalmology.* 2018:1120672117753704.

18. Jia Y, Ou T, Tokayer J, et al. Split-spectrum amplitude-decorrelation angiography with optical coherence tomography. *Optics Express.* 2012;20(4):4710-4725.

19. Weinhaus RS, Burke JM, Delori FC, Snodderly DM. Comparison of fluorescein angiography with microvascular anatomy of macaque retinas. *Experimental Eye Research.* 1995;61(1):1-16.

20. Alterman M, Henkind P. Radial peripapillary capillaries of the retina. II. Possible role in Bjerrum scotoma. *British Journal of Ophthalmology.* 1967;52(1):26-31.

21. Bonnin S, Mane V, Couturier A, et al. NEW INSIGHT INTO THE MACULAR DEEP VASCULAR PLEXUS IMAGED BY OPTICAL COHERENCE TOMOGRAPHY ANGIOGRAPHY. *Retina (Philadelphia, Pa).* 2015;35(11):2347-2352.

22. Jia Y, Bailey ST, Wilson DJ, et al. Quantitative optical coherence tomography angiography of choroidal neovascularization in age-related macular degeneration. *Ophthalmology.* 2014;121(7):1435-1444.

23. Agemy SA, Scripsema NK, Shah CM, et al. RETINAL VASCULAR PERFUSION DENSITY MAPPING USING OPTICAL COHERENCE TOMOGRAPHY ANGIOGRAPHY IN NORMALS AND DIABETIC RETINOPATHY PATIENTS. *Retina (Philadelphia, Pa).* 2015;35(11):2353-2363.

24. Liang MC, Witkin AJ. Optical Coherence Tomography Angiography of Mixed Neovascularizations in Age-Related Macular Degeneration. *Developments in ophthalmology.* 2016;56:62-70.

25. Miere A, Querques G, Semoun O, El Ameen A, Capuano V, Souied EH. OPTICAL COHERENCE TOMOGRAPHY ANGIOGRAPHY IN EARLY TYPE 3 NEOVASCULARIZATION. *Retina (Philadelphia, Pa).* 2015;35(11):2236-2241.

26. Srour M, Querques G, Semoun O, et al. Optical coherence tomography angiography characteristics of polypoidal choroidal vasculopathy. *The British journal of ophthalmology.* 2016;100(11):1489-1493.

27. Bulut M, Kurtuluş F, Gözkaya O, et al. Evaluation of optical coherence tomography angiographic findings in Alzheimer's type dementia. *British Journal of Ophthalmology.* 2017:bjophthalmol-2017-310476.

Tables

Table 1. Vessel density (X±SD) of various sections based on a ring centering on macula in four retinal layers.

	Whole (%)	Fovea (%)	Para (%)	T (%)	S (%)	N (%)	I (%)
Superficial	44.32±1.65	22.53±4.43	46.12±1.66	46.07±1.52	45.87±2.80	46.29±2.11	46.28±2.42
Deep	50.05±2.43	21.47±4.21	53.95±2.65	54.07±2.53	53.86±2.42	53.95±2.36	54.08±4.50
Outer retina	42.99±3.87	65.59±3.92	39.6±3.85	38.98±4.08	39.84±4.34	39.21±4.63	40.41±3.34
Choroid Cap	68.19±0.75	70.42±1.28	68.09±0.82	68.49±1.81	67.78±1.27	68.48±1.04	67.61±1.05

*Whole En-face(Whole), fovea, parafovea(Para), temporal (T), superior (S), nasal (N), inferior (I).

Table 2. Normative Vessel Density (X±SD) of various sections in the nerve head and the radial peripapillary capillary network.

	Whole (%)	ID (%)	Peri (%)	N (%)	I (%)	IT (%)	ST (%)	SN (%)	T (%)
erve ead	50.78±4.66	44.11±4.88	54.20±5.60	48.97±6.04	57.27±6.03	62.12±1.43	58.87±4.70	55.30±5.93	53.54±7.07
PC	48.43±3.16	33.13±4.15	54.94±4.97	49.72±6.06	56.86±5.60	62.41±1.19	61.23±5.84	52.96±4.40	55.84±5.88

*Whole En-face(Whole), peripapillary(Peri), Inside disc (ID), Nasal (N), Inferior nasal (IN), Inferior temporal (IT), Superior temporal (ST), superior nasal (SN), temporal (T).

Figures

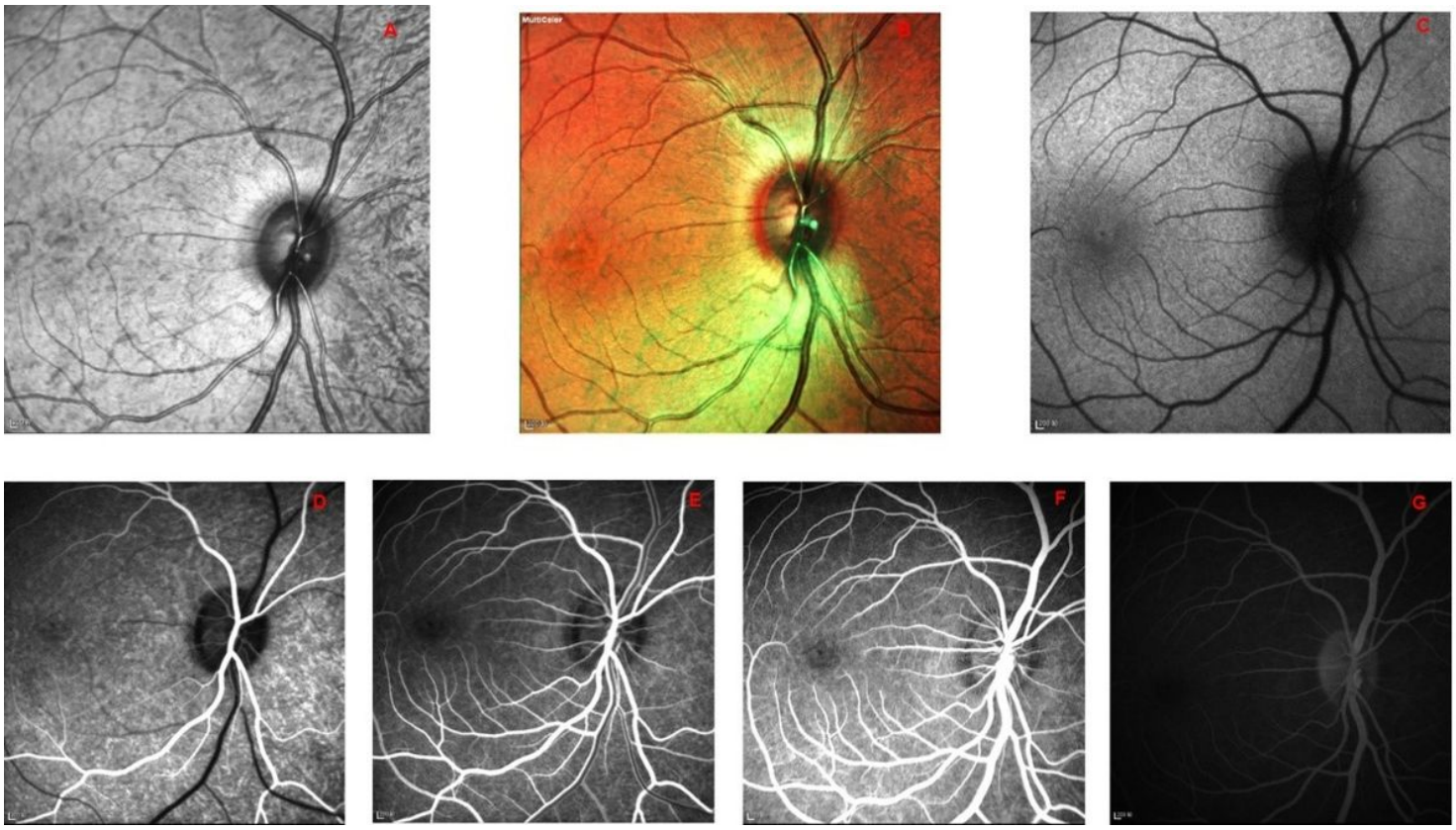

Figure 1

(A)IR image of normal cynomolgus macaque. (B) Multi-color image. (C) AF image. fluorescence angiography of cynomolgus macaque in (D)arterial stage, (E) arteriovenous stage, (F)venous stage, and (G) later stage.

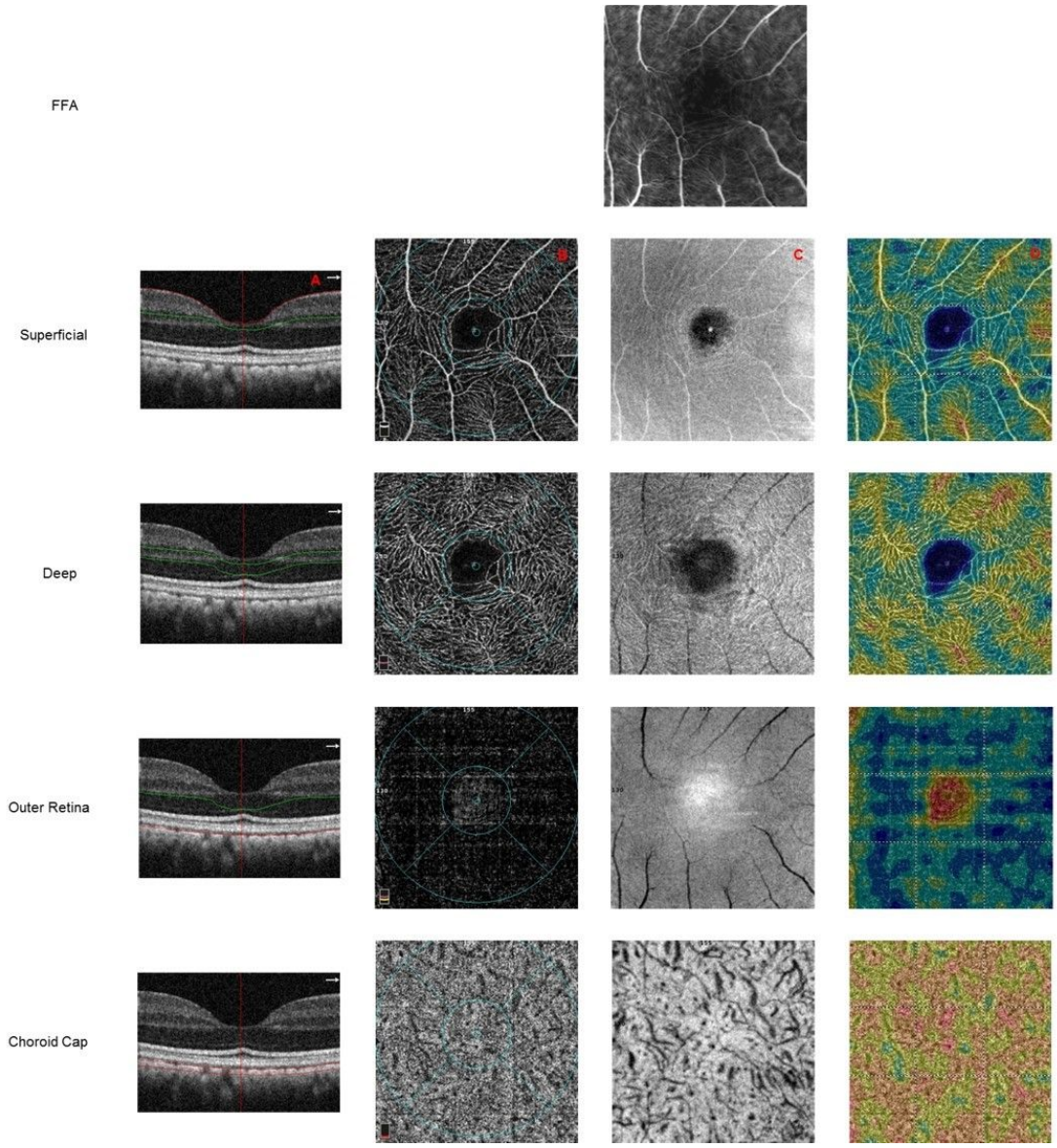

Figure 2

The fluorescence angiography（FFA）image of capillary plexuses in the macular and surrounding region matched with the optical coherence tomography angiography images. Optical coherence tomography angiography of the four capillary plexuses (A) Retinal layer in optical Coherence tomography. (B) Ring centering on macula with foveal ring (1 mm), four quadrants (superior, inferior, temporal, and nasal, 3mm). (C) The En-face images. (D) Normal virtual colored macular vascular density (Dark blue to red areas indicate areas of no flow to high flow density).

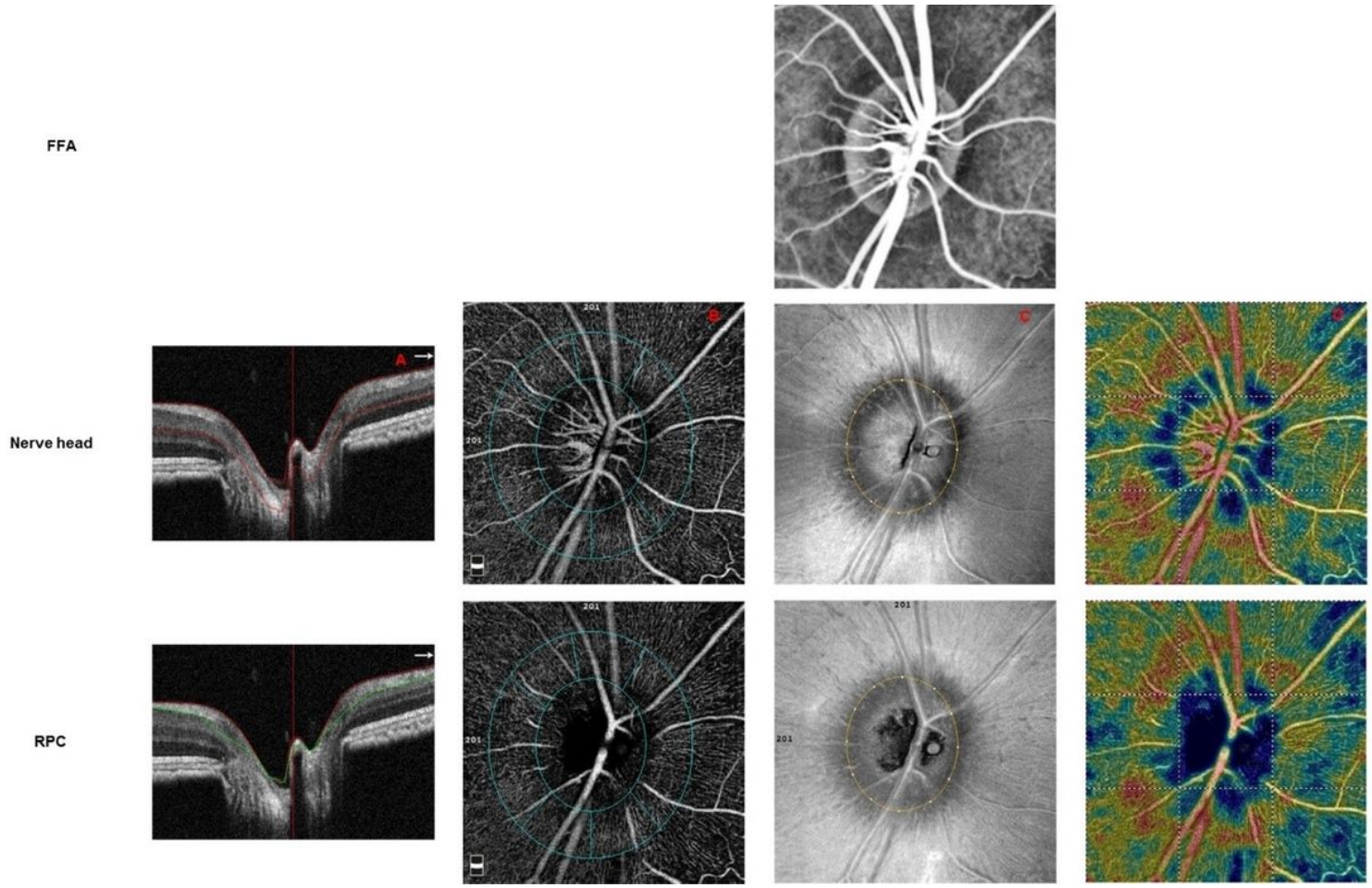

Figure 3

The fluorescence angiography（FFA）image of capillary plexuses in the optic disc and surrounding region matched with the optical coherence tomography angiography images. Optical coherence tomography image in the optic disc and surrounding region of nerve head layer and radial peripapillary capillary network. (A) Retinal layer in optical Coherence tomography. (B) A ring with width of 0.75mm, centering on the disc, automatically divided the scanned area into seven sections. (C) The En-face image of same region. (D) Normal virtual colored optic disc vascular density (Dark blue to red areas indicate areas of no flow to high flow density).

Supplementary Files

This is a list of supplementary files associated with this preprint. Click to download.

- supplement1.pdf